



**Manchester
Metropolitan
University**

Zaabalawi, Azziza, Astley, Cai, Renshall, Lewis, Beards, Frances, Lightfoot, Adam P, Degens, Hans, Whitehead, Debra, Alexander, Yvonne ORCID logo ORCID: <https://orcid.org/0000-0001-7151-8649>, Harris, Lynda K and Azzawi, May ORCID logo ORCID: <https://orcid.org/0000-0001-6238-9777> (2019) Tetramethoxystilbene-Loaded Liposomes Restore Reactive-Oxygen-Species-Mediated Attenuation of Dilator Responses in Rat Aortic Vessels Ex vivo. *Molecules*, 24 (23). p. 4360.

Downloaded from: <https://e-space.mmu.ac.uk/624533/>

Version: Published Version

Publisher: MDPI AG

DOI: <https://doi.org/10.3390/molecules24234360>

Usage rights: Creative Commons: Attribution 4.0

Please cite the published version

<https://e-space.mmu.ac.uk>

1 Communication

2 **Tetramethoxystilbene-loaded liposomes restore**
3 **reactive oxygen species-mediated attenuation of**
4 **dilator responses in rat aortic vessels, *ex vivo*.**

5 **Azziza Zaabalawi**¹, **Cai Astley**¹, **Lewis Renshall**^{2,3,4}, **Frances Beards**^{2,3,4}, **Adam P. Lightfoot**⁵,
6 **Hans Degens**^{5,6}, **Debra Whitehead**⁷, **Yvonne Alexander**¹, **Lynda K Harris**^{2,3,4}, **May Azzawi**^{1*}.

7 ¹ Centre for Bioscience, Faculty of Science and Engineering, Manchester Metropolitan University, Chester
8 Street, Manchester, M1 5GD.

9 ² Division of Pharmacy and Optometry, University of Manchester, Oxford Road, Manchester, M13 9PL.

10 ³ Maternal and Fetal Health Research Centre, Faculty of Biology, Medicine and Health, University of
11 Manchester, Oxford Road, Manchester, M13 9WL.

12 ⁴ Maternal and Fetal Health Research Centre, Manchester University NHS Foundation Trust, Manchester
13 Academic Health Sciences Centre, St Mary's Hospital, Manchester, M13 9WL.

14 ⁵ Centre for Musculoskeletal Science and Sports Medicine, Faculty of Science and Engineering, Manchester
15 Metropolitan University, Chester Street, Manchester, M1 5GD.

16 ⁶ Lithuanian Sports University, Kaunas.

17 ⁷ Advances Materials and Surface Engineering Research Centre, Faculty of Science and Engineering,
18 Manchester Metropolitan University, Chester Street, Manchester, M1 5GD.

19

20 * Correspondence: M.Azzawi@mmu.ac.uk

21 Received: date; Accepted: date; Published: date

22 **Abstract:** The methylated analogue of the polyphenol Resveratrol (RV), 2, 3', 4, 5'-
23 Tetramethoxystilbene (TMS) displays potent antioxidant properties and is an effective Cytochrome
24 P450 (CYP) 1B1 inhibitor. The bioavailability of TMS is low. Therefore, the use of liposomes for the
25 encapsulation of TMS is a promising delivery modality for enhanced uptake into tissues. We
26 examined the effect of delivery of TMS in liposomes, on the restoration of vasodilator responses of
27 isolated aortic vessels after acute tension elevation, *ex vivo*. Aortic vessels from young male Wistars
28 were isolated and endothelial-dependent (acetylcholine, ACh) and independent (sodium
29 nitroprusside, SNP) responses assessed. Acute tension elevation (1 hour) significantly reduced ACh
30 dilator responses, which were restored following incubation with superoxide dismutase or
31 apocynin (an NADPH oxidase inhibitor). Incubation with TMS-loaded liposomes (mean diameter
32 157 ± 6 nm; PDI 0.097) significantly improved the attenuated dilator responses following tension
33 elevation. Endothelial denudation or co-incubation with L-NNA (N ω -nitro-L-arginine; nitric oxide
34 synthase inhibitor) resulted in loss of dilator function. Our findings suggest that TMS-loaded
35 liposomes can restore attenuated endothelial-dependent dilator responses, induced by an oxidative
36 environment, by reducing NADPH oxidase-derived ROS and potentiating the release of the
37 vasodilator nitric oxide. TMS-loaded liposomes may be a promising therapeutic strategy to restore
38 vasodilator function in vascular disease.

39 **Keywords:** liposomes; 2, 3', 4, 5'-Tetramethoxystilbene; endothelium; aorta; oxidative stress;
40 reactive oxygen species; nitric oxide; vascular function.

41

42

43

44

45 1. Introduction

46 The vascular endothelial lining of blood vessels plays a pivotal role in the synthesis and release
47 of highly regulated vasoactive substances, including the potent vasodilator nitric oxide (NO). An
48 imbalance in the release of endothelial-derived vasodilator and vasoconstrictor mediators causes
49 endothelial dysfunction (ED), that results in a dominant pro-vasoconstrictor state due to the
50 generation of reactive oxygen species (ROS) and consequent reduction in NO bioavailability [1, 2].
51 ED is also associated with increased constriction, partly attributed to the decline in NO-mediated
52 inhibition of potent vasoconstrictors, such 20-hydroxyeicosatetraenoic acid (20 HETE). The latter is
53 a Cytochrome P450 (CYP) 1B1 eicosanoid, which has been shown to contribute to the development
54 of hypertension [3]. Attractive supplements to current treatment strategies include plant-derived
55 polyphenols such as Resveratrol (RV; 3, 5, 4'-trihydroxystilbene), due to its anti-oxidant properties
56 and ability to regulate the endothelial nitric oxide synthase enzyme [eNOS] [4, 5]. Recent studies
57 have been dedicated to developing derivatives of RV that have greater bioavailability and
58 pharmacological activity than RV [6]. In particular, the methylated derivative of RV; 2, 3', 4, 5'-
59 Tetramethoxystilbene (TMS), has been demonstrated to be 1000 times more potent in inhibiting
60 CYP1B1 than RV in spontaneously hypertensive rats (SHR) [7]. Elevated CYP1B1 activity,
61 endothelial dysfunction, ROS generation, NADPH oxidase activity and expression of NOX-1, ERK1
62 / 2 and p38 MAPK were diminished by TMS in the aorta, heart and kidney of the SHR model [7, 8].
63 Intravenous administration of TMS in rats shows moderate clearance (46.5 ± 7.6 mL / min / kg) [9]
64 and better bioavailability (4.5%) [10], compared to RV, however, the absolute oral bioavailability of
65 TMS remains low ($6.31 \pm 3.30\%$) [9].

66 Liposomes are recognised as promising agents for drug delivery due to their biocompatibility
67 and ability to cross physiological barriers [11, 12]. Liposomes have been clinically approved for
68 medical applications, including anticancer treatment, owing to their higher therapeutic efficacy and
69 low cytotoxicity. Major progress was made in their clinical application with the development of
70 PEGylated liposomes. Displaying PEG (N-[amino (polyethylene glycol)]) on the liposomal surface
71 increases their circulation time by preventing opsonisation, uptake and elimination by phagocytes
72 [12]. TMS encapsulated in PEGylated liposomes could thus serve as an attractive delivery system
73 whilst preserving the stability of TMS and enhancing its bioavailability [13]. The aim of this study
74 was to assess the potential of TMS-loaded liposomes to restore reduced vasodilator capacity of
75 isolated aortic vessels exposed to acute tension elevation, *ex vivo*.

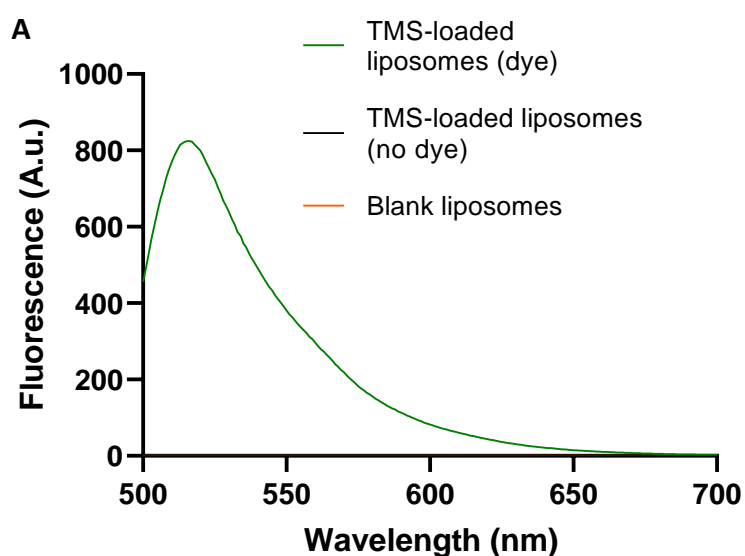
76 2. Results

77 2.1. Production and characterisation of TMS-loaded liposomes

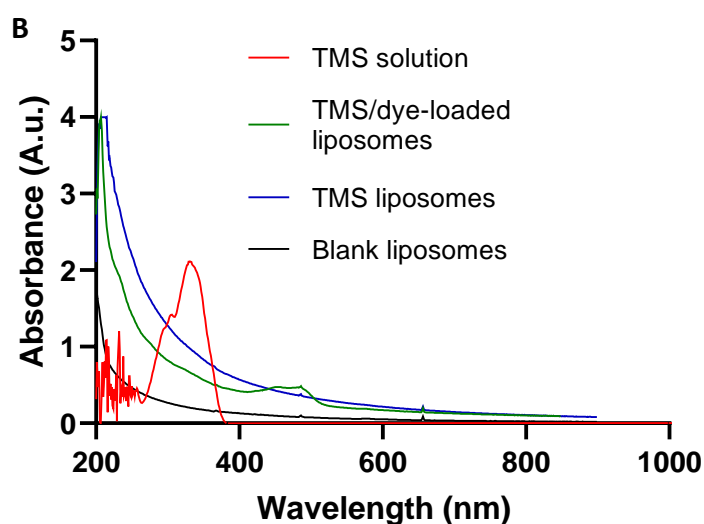
78 Phosphate buffered saline (PBS) containing liposomes (blank liposomes) had a mean diameter
79 of 182 ± 3 nm, polydispersity index (PDI) of 0.081 and an average zeta potential of -13.17 ± 0.76 mV.
80 TMS-loaded liposomes had a mean diameter of 157 ± 6 nm, PDI of 0.097 and an average zeta
81 potential of -13.13 ± 0.67 mV, whereas liposomes containing the dye, 5(6)-carboxyfluorescein and
82 TMS had a mean diameter of 150 ± 3 nm, PDI of 0.070 and an average zeta potential of -15.80 ± 1.31
83 mV. All measurements were conducted at pH 7.2-7.4.

84 Structural and functional characterisation of PEGylated liposomes were established using
85 chemical techniques to confirm dye and drug entrapment within the liposomes. Fluorescence peaks
86 were detected at 517 nm (corresponding to the dye) from TMS-dye encapsulated, but not blank or
87 TMS-loaded liposomes (Figure 1A). Independent analysis of TMS solution identified two
88 absorbance peaks at 302 and 326 nm, however, no peaks corresponding to TMS were
89 distinguishable in either TMS- or TMS-dye encapsulated liposomes (Figure 1B). TMS has a similar
90 infra-red profile to its well-characterised parent compound RV, with characteristic benzene valence
91 $\nu(\text{C}=\text{C})$ vibrations identifiable at 1588 and 1570 cm^{-1} . The strong, broad band characteristics of trans-

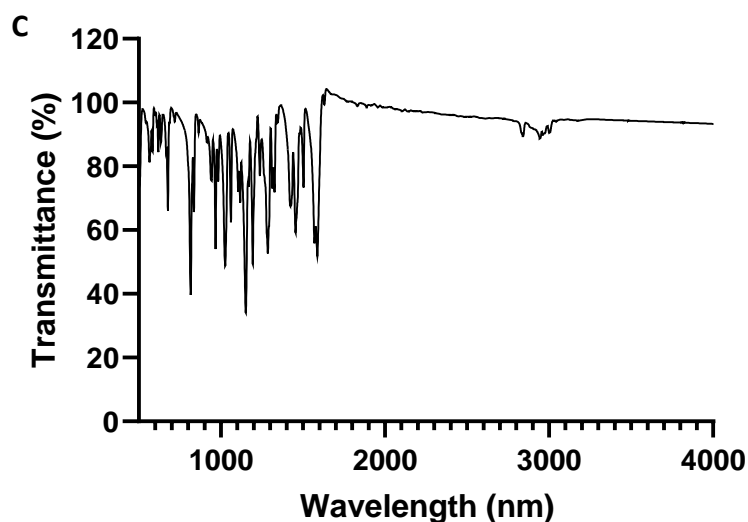
92 RV are noticeably absent between 3550-3200 cm^{-1} ; however, several bands are identifiable at 2850,
93 2952 and 3000 cm^{-1} , corresponding to the valence vibration and stretching of O-CH₃ bonds within
94 synthetically conjugated methyl groups. Additional CH₃ bending is observed at 1455 cm^{-1} . Ether
95 bonds (C-O-C) originating from phenolic groups are identifiable at 1026, 1152, 1195 and 1287 cm^{-1} .
96 The presence of TMS could not be identified in the liposomes due to the absence of corresponding
97 peaks. The individual components of the liposomal structure, 1,2-distearoyl-sn-glycero-3-
98 phosphocholine and 1,2-distearoyl-sn-glycero-3-phosphoethanolamine-N-[methoxy(polyethylene
99 glycol)-2000] ammonium salt were identifiable with peaks at 2950-2850 and 1730 cm^{-1} ,
100 corresponding with the presence of alkane (C-H) and carbonyl ester groups (C=O). The broad peak
101 observed at 3500 cm^{-1} are a result of OH groups found within fatty acids (cholesterol). Additional
102 vibrations corresponding with a C-C bond at 1248 cm^{-1} and a C-O bond from the phenolic group at
103 1154 cm^{-1} were identified within the spectrum (Figure 1C, D).



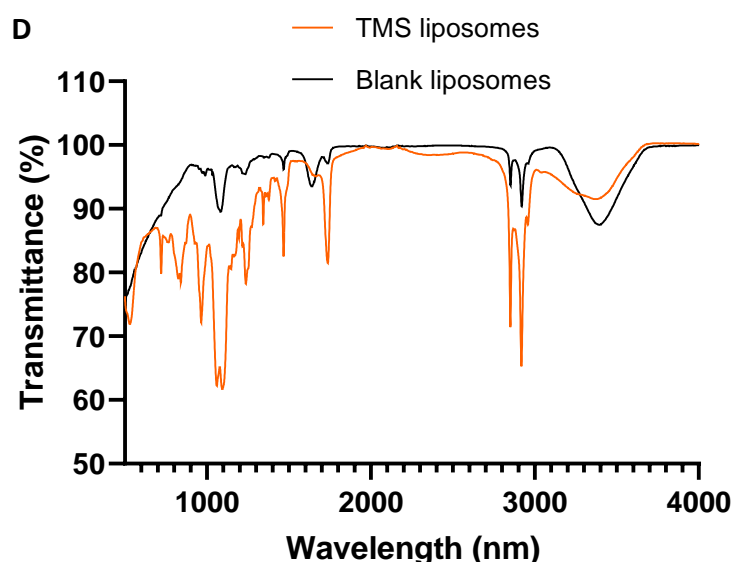
104



105



106

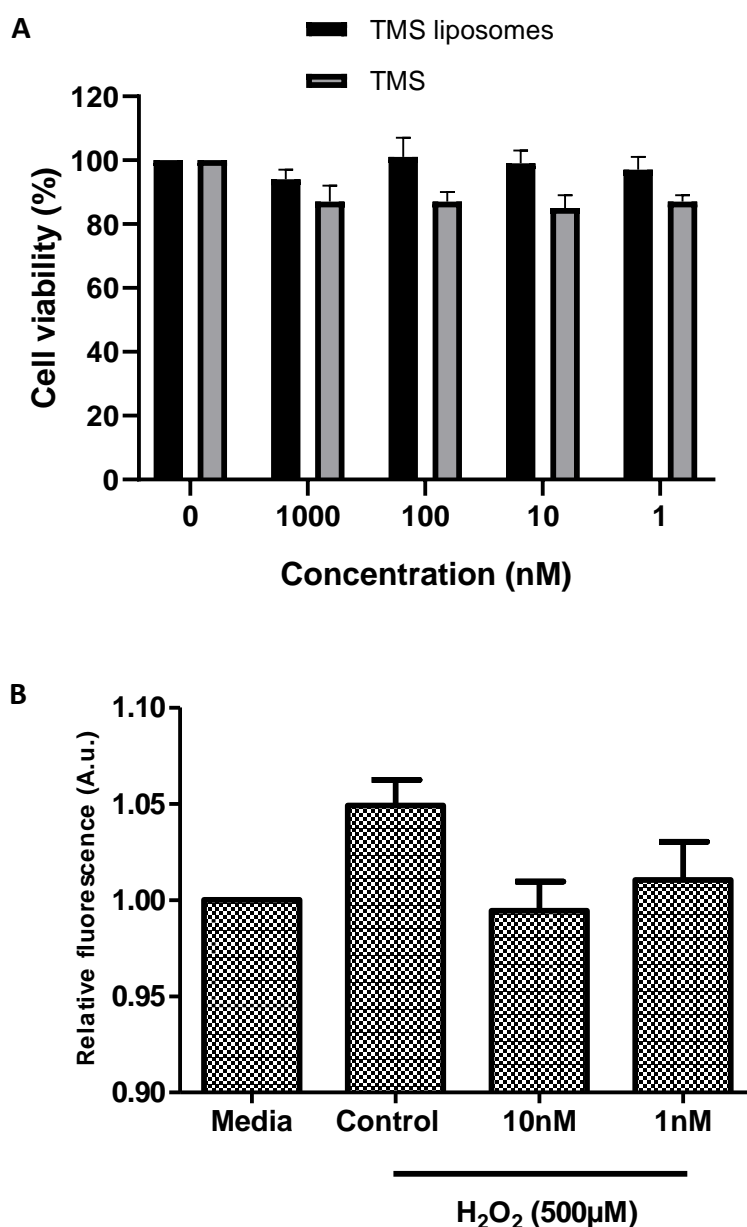


107

108 **Figure 1.** Chemical characterisation of tetramethoxystilbene (TMS) and TMS - loaded liposomes.
109 Fluorescence - spectroscopy displaying spectra between 500 – 700 nm (A). Ultraviolet - visible
110 spectroscopy (UV - Vis) displaying absorbance spectra between 200 – 1000 nm (B). Fourier -
111 transform infrared spectroscopy (FTIR) profile of TMS - powder (C) and TMS - loaded liposomes
112 (D) displaying transmittance (%) ranging between 500 – 4000 nm.

113 2.2. TMS-loaded liposomes maintain cell viability, *in vitro*

114 Human coronary artery endothelial cell (HCAEC) viability did not differ significantly between
115 control cells and cells incubated with TMS or TMS-loaded liposomes for 24 hours (Figure 2A). Drug
116 encapsulation within liposomes has previously been shown to provide greater therapeutic efficacy
117 with low cytotoxicity levels in human retinal endothelial cells [14]. In order to replicate elevated
118 superoxide levels observed in the vasculature during oxidative stress, HCAECs were stimulated
119 with hydrogen peroxide (H₂O₂) [15]. A reduction in fluorescence intensity, hence mitochondrial
120 superoxide production, was observed following incubation in TMS-loaded liposomes (Figure 2B).



121

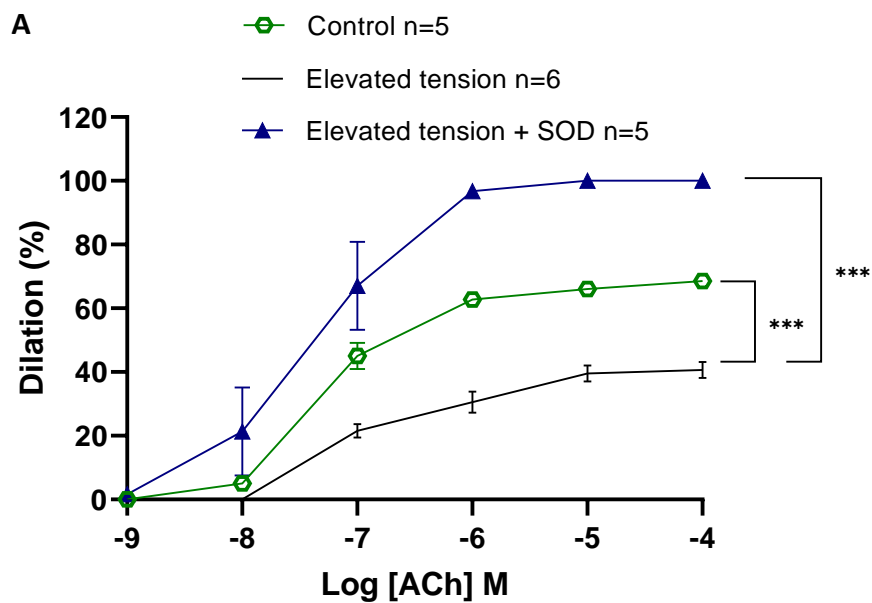
122

123 **Figure 2.** *In vitro* studies. Alamar blue cell viability assay performed in a 96 - well plate following
 124 administration of cumulative doses of tetramethoxystilbene (TMS) and TMS - loaded liposomes for
 125 24 hours (A). Mitochondrial superoxide generation in human coronary artery endothelial cells
 126 measured using MitoSOX Red reagent. Assays performed in a 96 - well plate with cells treated with
 127 TMS - loaded liposomes for 24 hours, followed by hydrogen peroxide (H_2O_2) 500 μM exposure.
 128 Untreated cells received media alone (B). Data are presented as mean \pm standard error of mean, n =
 129 3.

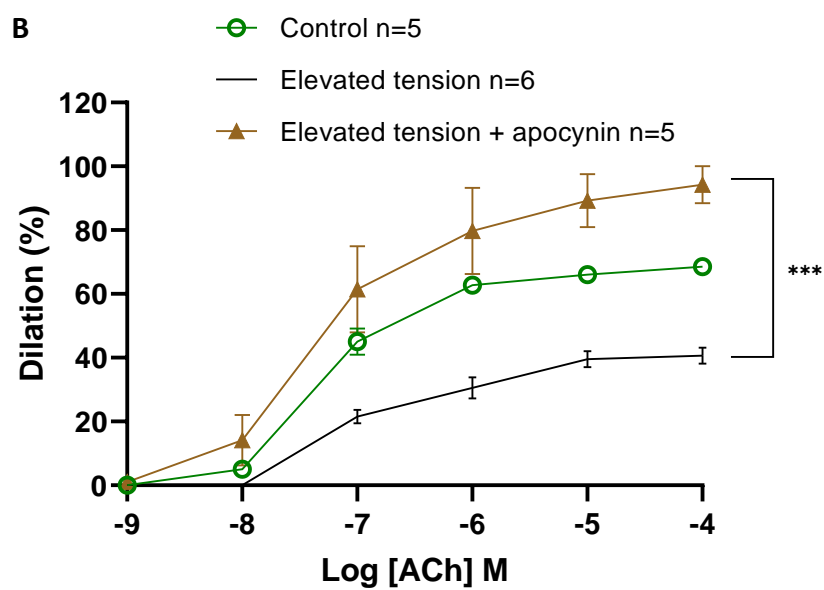
130 2.3. TMS-loaded liposomes restore endothelium-dependent dilation via Nitric oxide

131 All vessels constricted to high potassium (KPSS, 60 mM) and phenylephrine (Phe) (10^{-5} M)
 132 solution. Acute tension elevation significantly attenuated endothelium-dependent dilation to
 133 acetylcholine (ACh), which was restored following co-incubation with superoxide dismutase
 134 (Figure 3A) or the NADPH oxidase inhibitor, apocynin (Figure 3B). This reduction in dilation
 135 following tension elevation was significantly potentiated after incubation in TMS or TMS-loaded
 136 liposomes. Incubation with blank liposomes did not alter ACh dilator responses (Figure 3C). There

137 was a significant reduction in dilator responses following inhibition of nitric oxide synthesis by L-
138 NNA (Figure 3D). Vessels did not dilate to ACh following acute tension elevation and incubation
139 with TMS or TMS-loaded liposomes after endothelial denudation (Figure 3E). TMS and TMS-
140 loaded liposomes had no effect on endothelial-independent (SNP) dilation (data not shown).

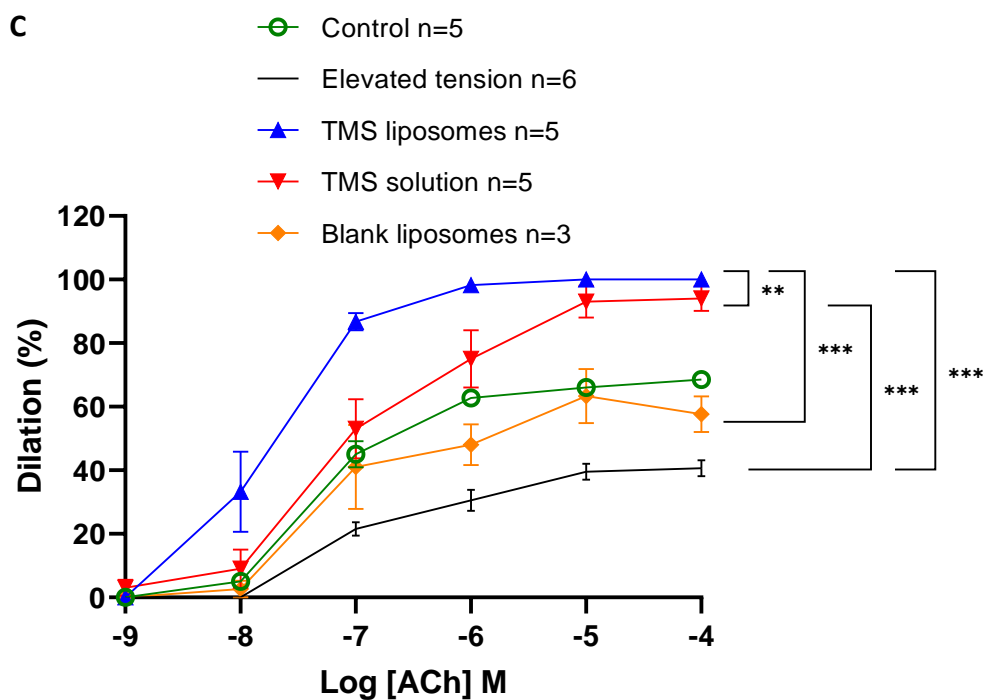


141

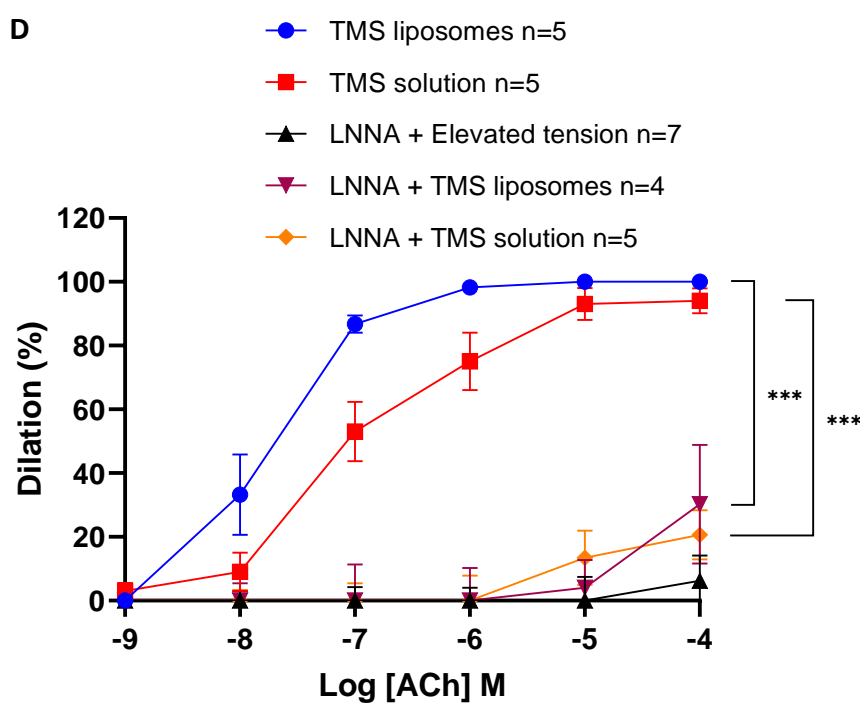


142

143

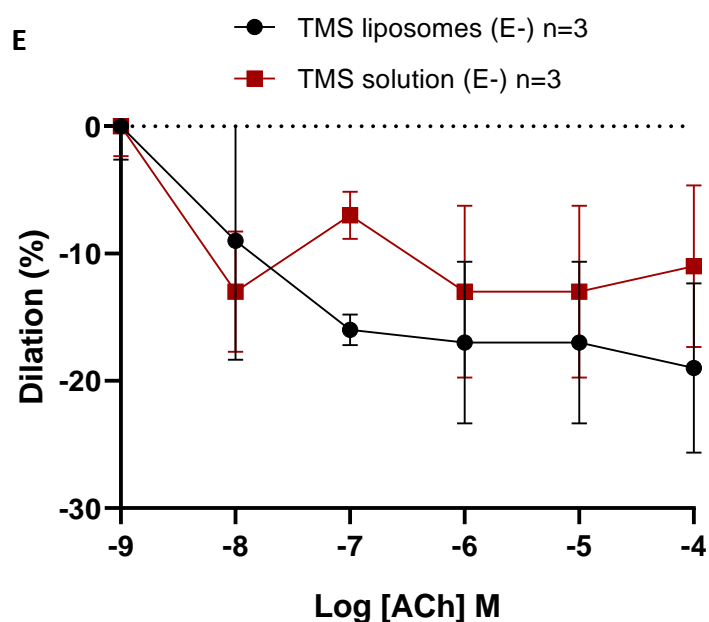


144



145

146



147

148 **Figure 3.** Vascular responses. Endothelium - dependent acetylcholine (ACh) responses in control
 149 vessels (control - 2g tension), following acute tension elevation (4g), acute tension elevation +
 150 superoxide dismutase (SOD) (A) and tension elevation + apocynin (B) in phenylephrine pre-
 151 constricted aortic vessels, *ex vivo*. The influence of tetramethoxystilbene (TMS), TMS - loaded
 152 liposomes and blank liposomes (C), the inhibitor N ω - nitro - L-arginine (LNNA) (D) and
 153 endothelial denudation (E) on endothelium - dependent ACh responses following acute tension
 154 elevation in phenylephrine pre-constricted aortic vessels, *ex vivo*. ** = P < 0.01, *** = P < 0.001. Error
 155 bars = standard error.

156 3. Discussion

157 We demonstrate that TMS, loaded within liposomes, can restore the reduced aortic vasodilator
 158 response, induced by a high oxidative environment, by potentiating the NO pathway. We produced
 159 TMS-loaded liposomes for direct uptake into the vasculature. These were characterised and dye
 160 loading confirmed using a range of chemical techniques. Due to the limited content that can be
 161 encapsulated within liposomes, a substantial absorbance peak would not be expected and may,
 162 therefore, be obscured by more prominent absorption peaks, as seen at 207 nm. This intense
 163 absorption towards the lower detection range has previously been observed in liposome samples
 164 and has been attributed to the presence of cholesterol. Cholesterol and other well-known oxysterols
 165 have been shown to absorb light at approximately 195 nm (vacuum-UV region). However, light
 166 scattering results in the λ max shifting towards a longer wavelength, producing an effect commonly
 167 referred to as false-energy. This results in a spectral 'redshift', with spectra now appearing in the
 168 207 nm region [16]. Using FTIR we identified several peaks which corresponded with the parent
 169 compound RV, confirming its derived nature. FTIR also confirmed the presence of constituent
 170 compounds used to synthesise the liposomes; however, the spectrographic profile for TMS was not
 171 distinguishable. Similar observations have been reported previously by several research groups,
 172 where nanoparticles are capable of obscuring the absorption peaks of encapsulated drugs, showing
 173 only the predominant parent compounds [17]. In the context of polyphenolic compounds, the
 174 presence of OH groups are commonplace and would be expected at around 3500 cm⁻¹. Despite
 175 being synthesised from a polyphenolic parent compound, it is crucial to note that in TMS, OH
 176 groups have been substituted for synthetically conjugated methyl groups, and as a result would not
 177 expect valance vibration bands at 3500 cm⁻¹. This, in addition to the presence of the same broad
 178 peak on blank liposomes are suggestive that the vibration observed are solely from the lipid

179 components. The distribution and intensity of absorption (% transmission) bands (blank vs. TMS-
180 loaded liposome) are a direct reflection of the range and quantity of chemical bonds present within
181 a given sample. In some instances, this may reflect an increase or decrease in band intensity, as a
182 result of sample modification and altered chemical composition. In this case, however, differences
183 in intensity observed between samples can be attributed to different dilution ratios of stock
184 samples.

185 Using isolated HCAECs in culture, we demonstrate that TMS-loaded liposomes can maintain
186 cell viability. When the cells were exposed to H₂O₂, mitochondrial superoxide generation was
187 reduced following 24 hour incubation with TMS-loaded liposomes. The lack of significance in
188 reduction suggests that TMS-loaded liposomes may quench additional sources of ROS, including
189 cytosolic superoxide, due to NADPH oxidase stimulation and NOS uncoupling [15]. Furthermore,
190 TMS-loaded liposomes may also influence the upregulation of antioxidant enzymes and eNOS
191 expression in a similar way to resveratrol [18, 19]. To demonstrate the vasodilator potential of the
192 TMS-loaded liposomes, we used aortic vessels, exposed to elevated tension, to generate an
193 oxidative environment. The upregulation of ROS sources particularly NADPH oxidase, decreases
194 SOD activity and causes eNOS uncoupling [2]. Vessel incubation with the NADPH oxidase
195 inhibitor apocynin significantly potentiated dilator responses following tension elevation. This is
196 consistent with previous findings that NADPH oxidase is the major ROS generator in the
197 vasculature [20]. Apocynin blocks the translocation of p47phox to the membrane, hence preventing
198 the release of NADPH oxidase-derived superoxide [21].

199 Vessel incubation with TMS / TMS-loaded liposomes restored endothelium-dependent dilator
200 responses following tension elevation even beyond the maximal dilation observed in control
201 vessels. TMS has been documented to reduce the increase in NADPH oxidase-derived ROS in
202 aortic, mesenteric and renal arteries of spontaneously hypertensive rats (SHR) primarily via
203 inhibition of CYP1B1 activity. CYP1B1 has been reported to contribute to ED in SHR, with TMS
204 reversing this effect as indicated by improvement in vasodilation in response to ACh [7]. It appears
205 that ED in SHR and DOCA hypertensive models occurs largely as a result of elevated ROS
206 generation, resulting from Arachidonic Acid (AA) metabolites such as 20-HETE that is produced by
207 CYP1B1. This subsequently elevates NADPH oxidase activity and ROS levels resulting in the
208 activation of signalling molecules including ERK1 / 2, p38 MAPK and c-Src [22]. This was prevented
209 by TMS treatment [8]. The potentiation in dilator responses demonstrated by TMS can be
210 attributable to increased eNOS phosphorylation, reduced NADPH oxidase-derived ROS and eNOS
211 uncoupling via CYP1B1 inhibition, direct quenching of ROS and the activation of SIRT1 and / or
212 AMPK pathway leading to elevated NO bioavailability. Inhibition of NO synthesis using L-NNA
213 significantly attenuated the restored vasodilation by TMS / TMS-liposomes, suggesting its
214 mechanism of action is mainly mediated via the NO pathway, which plays a major role in the
215 maintenance of basal vasomotor tone in conduit vessels under normal but also under hypertensive
216 conditions [23]. The dilator potential of TMS / TMS-liposomes was lost in denuded vessels, further
217 suggesting that the potentiated dilation is mainly mediated via endothelial dependent mechanisms.
218 The potentiation of dilator capacity by TMS-loaded liposomes to a higher extent than TMS solution,
219 may be due to increased cellular uptake of liposomes, enhanced solubility and sustained release of
220 encapsulated TMS [12] as compared to the rapid depletion / washout of TMS solution in the
221 experimental setup. Therefore, we propose that the enhanced dilator effects of TMS-loaded
222 liposomes is retained due to slow continued release of encapsulated TMS that has already been
223 taken up by the cells.

224 4. Conclusion

225 In the present study, we exposed isolated aortic vessels to elevated tension, *ex vivo*, to generate
226 an oxidative environment, in order to examine the effects of TMS-loaded liposomes in restoring
227 dilator capacity. We demonstrate that TMS-loaded liposomes can restore the attenuated

228 endothelial-dependent dilator responses, by reducing NADPH oxidase-derived ROS and
229 potentiating NO mediated dilation. TMS-loaded liposomes may thus be a promising therapeutic
230 strategy to improve vasodilator function in vascular disease.

231 5. Materials and Methods

232 5.1. Chemicals, Reagents and Materials

233 2, 3', 4, 5'-Tetramethoxystilbene (TMS) and all reagents were purchased from Sigma-Aldrich,
234 UK. Physiological salt solution (PSS) had the following composition [mM]: 119 NaCl, 4.7 KCl, 1.2
235 MgSO₄·7H₂O, de-ionised (dH₂O), 25 NaHCO₃, 1.17 KHPO₄, 0.03 K₂EDTA, 5.5 glucose, 1.6 CaCl₂·H₂O;
236 pH 7.4.

237 5.2. Liposome Synthesis and Characterisation

238 Liposomes were synthesised using the thin lipid film process as previously described [24, 25].
239 Briefly, the constituent lipids 1,2-distearoyl-*sn*-glycero-3-phosphocholine (DSPC; 32.5 mM, Avanti
240 Polar Lipids), 1,2-distearoyl-*sn*-glycero-3-phosphoethanolamine-*N*-[methoxy(polyethylene glycol)-
241 2000] ammonium salt [DSPE-PEG(200); 1.875 mM, Avanti Polar Lipids] and cholesterol (15 mM,
242 Sigma Aldrich) were dissolved in 5 ml of chloroform in a round-bottom flask. Subsequent rotary
243 evaporation (40°C, 270 mbar) removed excess chloroform and the lipid film was placed in a
244 vacuum oven overnight (25°C, 0 mbar). The thin film was rehydrated with 1 ml of PBS, vortexed for
245 10 minutes, heated to 55°C and vortexed for 5 minutes at 1 hour intervals for a minimum of 4 hours.
246 The suspension containing large multilamellar vesicles was then extruded 11 times using a 1 ml
247 Mini-Extruder (Avanti Polar Lipids) through a 200 nm polycarbonate membrane to produce
248 unilamellar liposomes ~200 nm in diameter. To remove impurities, dialysis against PBS (8 x 500 ml;
249 24 hours) in a Slide-A-Lyzer cassette with a molecular weight cutoff of 3.5 kD (Thermo Fisher
250 Scientific) was performed. Liposomes were then stored at 4°C until use. The size distribution and
251 polydispersity index of liposomes were measured by dynamic light scattering (DLS; 25°C;
252 scattering angle of 173° Zetasizer Nano ZS, Model ZEN3600, Malvern Instruments). For TMS-
253 loaded liposomes, the lipid film was rehydrated with 1 ml TMS (2 mM in PBS) heated to 55°C and
254 extruded / dialysed as above, to give a final encapsulated concentration of approximately 1 mM
255 TMS. For dual-loaded TMS / 5(6)-carboxyfluorescein liposomes a 1ml solution of TMS (2 mM)
256 containing 5(6)-carboxyfluorescein (5.3 mM) was used to rehydrate the lipid film, to give a final
257 concentration of 1 mM and 2.65 mM, respectively. UV-Vis spectrophotometer (Jenway 7305, Cole-
258 Palmer) and fluorescence spectrometer (F-7000, Hitachi) was used to determine absorption and
259 fluorescence spectra, respectively. The structure of liposomes was assessed using FTIR (Nicolet 380
260 FT-IR Spectrometer, Thermo Scientific).

261 5.3. Cell Culture Studies

262 HCAECs were purchased from PromoCell (Heidelberg, Germany). Cells were grown in
263 Endothelial Cell Growth Medium (MV2) supplemented with growth medium MV2 supplement
264 pack, 100 µl / mL penicillin and 100 µl / mL streptomycin. Cells were maintained at 37°C with 4%
265 CO₂ in a humidified incubator and subcultured 1:3 after reaching 80% confluency. The viability of
266 HCAECs was determined using the fluorometric Alamar Blue Cell Viability assay. HCAECs were
267 seeded in 96-well plates and exposed to increasing doses of TMS solution and TMS liposomes (1
268 nM- 1 µM) for 24 hours. Fluorescence was measured at *ex.* 570 / *em.* 590 nm using a BioTek Synergy
269 HT microplate reader. The generation of intracellular superoxide was quantified using MitoSOX
270 Red Mitochondrial Superoxide Indicator (Thermo, UK). Briefly, HCAECs were cultured on 96-well
271 plates at a density of 1 x 10⁴ cells / well for 24 hours. Cells were then incubated with TMS-loaded
272 liposomes (10 and 1 nM) for 24 hours, washed, then incubated with fresh medium in the presence
273 of 500 µM H₂O₂ for 30 minutes. Cells were incubated in the dark at 37°C with MitoSOX for 10

274 minutes. Fluorescence was measured at *ex.* 510 / *em.* 580 nm (BioTek Synergy HT microplate
275 reader).

276 5.4. Vascular Function Studies

277 Aortic vessels were excised from male Wistar rats (150-250 g) euthanized by stunning and
278 cervical dislocation, following Institutional guidelines and in accordance with the 'Animals
279 Scientific procedures act 1986'. The heart was isolated and kept in oxygenated PSS (95% O₂: 5% CO₂;
280 4°C) in a dissection dish. The aortic vessel was gently pinned down at both ends and the underlying
281 adipose tissue was removed using dissection scissors and forceps, under a binocular dissection
282 microscope with a fibre optic light source (Olympus SZ61). The vessel was then cut into 3 mm rings
283 and mounted between two fine steel wires in a calibrated organ-bath system, immersed in
284 oxygenated PSS at 35°C, then placed under 2g tension using Harvard isometric strain transducer
285 and tension recorded using Labchart 8 (Power lab, AD Instruments, UK), as previously described
286 [26]. The viability of blood vessels was examined by ascertaining initial responses to high
287 potassium solution (KPSS, 60 mM). Vessels that recorded constrictor responses of <1.0 g tension
288 were not considered viable and were excluded from the study. The influence of TMS / TMS-loaded
289 liposomes on blood vessel function was determined in response to vasodilator agonists including;
290 acetylcholine (ACh) (10⁻⁹M - 10⁻⁴M), sodium nitroprusside (SNP) (100 nM) and the vasoconstrictor,
291 Phenylephrine (Phe) (10⁻⁵M).

292 Endothelial-dependent (ACh) and independent (SNP) responses were examined following
293 acute tension elevation (4g, 1 hour) in the presence / absence of TMS / TMS-loaded liposomes. In
294 order to establish the minimal dose of TMS required to achieve maximal dilation, cumulative doses
295 of TMS (1 pM-10 mM) were added to pre-constricted vessels with Phe. In order to assess the dilator
296 effect of superoxide dismutase (SOD) and TMS / TMS-loaded liposomes, aortic rings were initially
297 placed under elevated tension (4 g, 1 hour), followed by a 30 minute incubation with SOD (300 U /
298 mL) or TMS / TMS-loaded liposomes (1 nM). Constrictor and dilator responses were investigated
299 and recorded. To evaluate the dilator component involved in the action of TMS / TMS-loaded
300 liposomes, inhibition studies were performed. LNNA (NO synthesis inhibitor; 100 µM) was used to
301 evaluate the influence of NO following acute tension elevation with and without incubation with
302 TMS / TMS-loaded liposomes. To assess the contribution of NADPH oxidase on the dilator function
303 of TMS / TMS-loaded liposomes, apocynin (0.3 mM, 30 minutes) was used to block NADPH
304 oxidase activity. Endothelial denudation was used to assess the endothelial dependent dilator
305 component of TMS / TMS-loaded liposomes. To investigate any effects of the liposomes alone on
306 vasodilation, aortic vessels were incubated with blank liposomes (drug-free) (1 nM) for 30 minutes
307 after tension elevation. Constrictor and dilator responses to Phe and ACh was measured,
308 respectively.

309 5.5. Statistical Analysis

310 All values are presented as mean ± standard error. Data were tested for normal distribution
311 using Shapiro-Wilk test. Results were analysed using a two-way ANOVA followed by Tukey's
312 multiple comparisons post-test (IBM SPSS Statistics 25). Statistical significance is P < 0.05. * = P <
313 0.05, ** = P < 0.01, *** = P < 0.001. P > 0.05 was considered non-significant.

314

315 **Author Contributions:** Conceptualization, MA, LKH; methodology, AZ, CA, LR, FB; formal analysis, AZ, CA;
316 investigation, AZ, CA; data curation, AZ, CA, LR, HD; writing—original draft preparation, AZ, CA, MA;
317 writing—review and editing, AZ, CA, MA, APL, HD, YA; DW; LKH; supervision, MA, LKH, HD, APL, YA,
318 DW; funding acquisition, MA, LKH, YA.

319 **Funding:** This work was supported by a Manchester Institute for Collaborative Research on Ageing (MICRA)
320 Seedcorn Award to MA, LKH, and YA. The Maternal and Fetal Health Research Centre is supported by funding

321 from Tommy's the Baby Charity, an Action Research Endowment Fund, the Manchester Biomedical Research
322 Centre and the Greater Manchester Comprehensive Local Research Network.

323

324 **Conflicts of Interest:** The authors declare no conflict of interest. The funders had no role in the design of the
325 study; in the collection, analyses, or interpretation of data; in the writing of the manuscript, or in the decision to
326 publish the results.

327

328

329 References-

- 330 1. Chen, W.; Druhan, L.; Chen, C.; Hemann, C.; Chen, Y.; Berka, V.; Tsai, A.; Zweier, J. Peroxynitrite
331 Induces Destruction of the Tetrahydrobiopterin and Heme in Endothelial Nitric Oxide Synthase:
332 Transition from Reversible to Irreversible Enzyme Inhibition. *Biochemistry* **2010**, *49* (14), 3129-3137.
- 333 2. Rodrigo, R.; González, J.; Paoletto, F. The Role of Oxidative Stress in the Pathophysiology of
334 Hypertension. *Hypertension Research* **2011**, *34* (4), 431-440.
- 335 3. Toth, P.; Csiszar, A.; Tucsek, Z.; Sosnowska, D.; Gautam, T.; Koller, A.; Schwartzman, M.; Sonntag, W.;
336 Ungvari, Z. Role Of 20-HETE, TRPC Channels, and Bkca in Dysregulation of Pressure-Induced Ca²⁺
337 Signaling and Myogenic Constriction of Cerebral Arteries in Aged Hypertensive Mice. *American*
338 *Journal of Physiology-Heart and Circulatory Physiology* **2013**, *305* (12), H1698-H1708.
- 339 4. Bonnefont-Rousselot, D. Resveratrol and Cardiovascular Diseases. *Nutrients* **2016**, *8* (5), 250.
- 340 5. Zordoky, B.; Robertson, I.; Dyck, J. Preclinical and Clinical Evidence for the Role of Resveratrol in the
341 Treatment of Cardiovascular Diseases. *Biochimica et Biophysica Acta (BBA) - Molecular Basis of Disease*
342 **2015**, *1852* (6), 1155-1177.
- 343 6. Nawaz, W.; Zhou, Z.; Deng, S.; Ma, X.; Ma, X.; Li, C.; Shu, X. Therapeutic Versatility of Resveratrol
344 Derivatives. *Nutrients* **2017**, *9* (11), 1188.
- 345 7. Jennings, B.; Montanez, D.; May, M.; Estes, A.; Fang, X.; Yaghini, F.; Kanu, A.; Malik, K. Cytochrome
346 P450 1B1 Contributes to Increased Blood Pressure and Cardiovascular and Renal Dysfunction in
347 Spontaneously Hypertensive Rats. *Cardiovascular Drugs and Therapy* **2014**, *28* (2), 145-161.
- 348 8. Sahan-Firat, S.; Jennings, B.; Yaghini, F.; Song, C.; Estes, A.; Fang, X.; Farjana, N.; Khan, A.; Malik, K.
349 2,3',4,5'-Tetramethoxystilbene Prevents Deoxycorticosterone-Salt-Induced Hypertension:
350 Contribution of Cytochrome P-450 1B1. *American Journal of Physiology-Heart and Circulatory Physiology*
351 **2010**, *299* (6), H1891-H1901.
- 352 9. Lin, H.; Zhang, W.; Go, M.; Tringali, C.; Spatafora, C.; Ho, P. Quantification of trans-3, 4, 5, 4'-
353 Tetramethoxystilbene in Rat Plasma by HPLC: Application to Pharmacokinetic Study. *Journal of*
354 *Agricultural and Food Chemistry* **2011**, *59* (4), 1072-1077.
- 355 10. Lin, H.; Choo, Q.; Ho, P. Quantification of Oxyresveratrol Analog Trans-2, 4, 3', 5'-
356 Tetramethoxystilbene in Rat Plasma by a Rapid HPLC Method: Application in a Pre-Clinical
357 Pharmacokinetic Study. *Biomedical Chromatography* **2010**, *24* (12), 1373-1378.
- 358 11. Hu, Y.; Gaillard, P.; Rip, J.; de Lange, E.; Hammarlund-Udenaes, M. In Vivo Quantitative
359 Understanding of Pegylated Liposome's Influence on Brain Delivery of Diphenhydramine. *Molecular*
360 *Pharmaceutics* **2018**, *15* (12), 5493-5500.
- 361 12. Janeczek, A.; Scarpa, E.; Horrocks, M.; Tare, R.; Rowland, C.; Jenner, D.; Newman, T.; Oreffo, R.; Lee,
362 S.; Evans, N. Pegylated Liposomes Associate with Wnt3a Protein and Expand Putative Stem Cells in
363 Human Bone Marrow Populations. *Nanomedicine* **2017**, *12* (8), 845-863.

- 364 13. Choi, Y.; Han, H. Nanomedicines: Current Status and Future Perspectives in Aspect of Drug Delivery
365 and Pharmacokinetics. *Journal of Pharmaceutical Investigation* **2017**, *48* (1), 43-60.
- 366 14. Arta, A.; Eriksen, A.; Melander, F.; Kempen, P.; Larsen, M.; Andresen, T.; Urquhart, A. Endothelial
367 Protein C-Targeting Liposomes Show Enhanced Uptake and Improved Therapeutic Efficacy in
368 Human Retinal Endothelial Cells. *Investigative Ophthalmology & Visual Science* **2018**, *59* (5), 2119.
- 369 15. Coyle, C.; Kader, K. Mechanisms of H₂O₂-Induced Oxidative Stress in Endothelial Cells Exposed to
370 Physiologic Shear Stress. *ASAIO Journal* **2007**, *53* (1), 17-22.
- 371 16. Gupta, U.; Singh, V.; Kumar, V.; Khajuria, Y. Spectroscopic Studies of Cholesterol: Fourier Transform
372 Infra-Red and Vibrational Frequency Analysis. *Materials Focus* **2014**, *3* (3), 211-217.
- 373 17. Pople, P.; Singh, K. Development and Evaluation of Colloidal Modified Nanolipid Carrier: Application
374 to Topical Delivery of Tacrolimus. *European Journal of Pharmaceutics and Biopharmaceutics* **2011**, *79* (1),
375 82-94.
- 376 18. Ungvari, Z.; Labinskyy, N.; Mukhopadhyay, P.; Pinto, J.; Bagi, Z.; Ballabh, P.; Zhang, C.; Pacher, P.;
377 Csizsar, A. Resveratrol Attenuates Mitochondrial Oxidative Stress in Coronary Arterial Endothelial
378 Cells. *American Journal of Physiology-Heart and Circulatory Physiology* **2009**, *297* (5), H1876-H1881.
- 379 19. Schmitt, C.; Heiss, E.; Dirsch, V. Effect of Resveratrol on Endothelial Cell Function: Molecular
380 Mechanisms. *BioFactors* **2010**, *36* (5), 342-349.
- 381 20. Drummond, G.; Selemidis, S.; Griendling, K.; Sobey, C. Combating Oxidative Stress in Vascular
382 Disease: NADPH Oxidases as Therapeutic Targets. *Nature Reviews Drug Discovery* **2011**, *10* (6), 453-471.
- 383 21. Viridis, A.; Gesi, M.; Taddei, S. Impact of Apocynin on Vascular Disease in Hypertension. *Vascular
384 Pharmacology* **2016**, *87*, 1-5.
- 385 22. Malik, K.; Jennings, B.; Yaghini, F.; Sahan-Firat, S.; Song, C.; Estes, A.; Fang, X. Contribution of
386 Cytochrome P450 1B1 to Hypertension and Associated Pathophysiology: A Novel Target for
387 Antihypertensive Agents. *Prostaglandins & Other Lipid Mediators* **2012**, *98* (3-4), 69-74.
- 388 23. Kang, K. Endothelium-Derived Relaxing Factors of Small Resistance Arteries in Hypertension.
389 *Toxicological Research* **2014**, *30* (3), 141-148.
- 390 24. Cureton, N.; Korotkova, I.; Baker, B.; Greenwood, S.; Wareing, M.; Kotamraju, V.; Teesalu, T.; Cellesi,
391 F.; Tirelli, N.; Ruoslahti, E.; Aplin, J.; Harris, L. Selective Targeting of a Novel Vasodilator to the Uterine
392 Vasculature to Treat Impaired Uteroplacental Perfusion in Pregnancy. *Theranostics* **2017**, *7* (15), 3715-
393 3731.
- 394 25. King, A.; Ndifon, C.; Lui, S.; Widdows, K.; Kotamraju, V.; Agemy, L.; Teesalu, T.; Glazier, J.; Cellesi,
395 F.; Tirelli, N.; Aplin, J.; Ruoslahti, E.; Harris, L. Tumor-Homing Peptides as Tools for Targeted Delivery
396 of Payloads to the Placenta. *Science Advances* **2016**, *2* (5), e1600349.
- 397 26. Farooq, A.; Shukur, A.; Astley, C.; Tosheva, L.; Kelly, P.; Whitehead, D.; Azzawi, M. Titania coating of
398 mesoporous silica nanoparticles for improved biocompatibility and drug release within blood vessels.
399 *Acta Biomater.* **2018**, *76*, 208-216.

400



© 2019 by the authors. Submitted for possible open access publication under the terms and conditions of the Creative Commons Attribution (CC BY) license (<http://creativecommons.org/licenses/by/4.0/>).

401